

Research Article

Equilibrium Isotherms, Kinetics, and Thermodynamic Mechanisms of a Novel Polyacrylamide-*Strychnos potatorum* Seed-Derived Activated Carbon Composite for Aqueous Hardness Removal

Yohan L. N. Mathota Arachchige  and T. D. Fernando 

Department of Chemistry, University of Kelaniya, Kelaniya, Sri Lanka

Correspondence should be addressed to Yohan L. N. Mathota Arachchige; nadeesha@kln.ac.lk

Received 18 April 2022; Revised 16 July 2022; Accepted 21 July 2022; Published 24 September 2022

Academic Editor: Mohd Sajid Ali

Copyright © 2022 Yohan L. N. Mathota Arachchige and T. D. Fernando. This is an open access article distributed under the Creative Commons Attribution License, which permits unrestricted use, distribution, and reproduction in any medium, provided the original work is properly cited.

Hardness in water is responsible for both residential and industrial problems. Moreover, drinking hard water is suspected as the main cause of chronic kidney disease of unknown etiology (CKDu) in Sri Lanka. The major constituents that are responsible for water hardness are calcium and magnesium ions. In this study, a composite was synthesized using activated carbon of *Strychnos potatorum* seeds (ACSP) and acrylamide to remove hardness in drinking water. The synthesized composite was characterized using Fourier transform infrared-attenuated total reflection (FTIR-ATR) spectroscopy and scanning electron microscope (SEM). According to this study, the process of removal of hardness depends on the contact time, adsorbent dosage, initial contents, and pH of the solution. The adsorption data were well fitted to the Freundlich isotherm and the pseudo-second-order kinetic models. Furthermore, environmental samples collected from Anuradhapura, Sri Lanka, which is well known for water with high hardness, were treated with an adsorbent, and hardness was reduced effectively. Moreover, the adsorption appeared to be spontaneous in nature. Finally, it can be concluded that this adsorbent can be used as an effective hardness-removing agent.

1. Introduction

Hardness in water causes both residential and industrial issues. It produces hard scales in pipes and boilers [1]. Moreover, hard water causes toughening of skin and hair [2]. The major constituents that are responsible for water hardness are Ca and Mg ions. Those constituents originated in water by seepage of sedimentary rocks and runoff from soil [1, 3]. Hardness is expressed as milligrams of calcium carbonate equivalent per liter and that can be classified into four groups: the calcium carbonate concentration of water below 60 mg/L is generally considered as soft; 60–120 mg/L, moderately hard; 120–180 mg/L, hard; and more than 180 mg/L, very hard [3]. Groundwater is the main drinking water source in many countries. Therefore, the consumption of hard water causes serious health problems such as kidney problems, cancer, cardiovascular disorder, and urolithiasis [2].

Due to the problems faced by hardness, many researchers have focused on various methods for the removal of excess hardness from water and wastewater. Various techniques including nanofiltration [1, 4], ion exchange [5, 6], and electro-coagulation [7] have been widely used for the treatment of hardness-enriched water.

However, due to the high cost, applying these methods to remove hardness is not economical [2]. Moreover, there are limited studies focused on the removal of hardness by adsorption using low-cost materials [2, 8].

The seeds of the *Strychnos potatorum* trees are nontoxic [9, 10]. And also, due to the water purification ability of seeds, that tree is known as a clearing nut tree. This property is due to the presence of lipids, polyelectrolytes, carbohydrates, and alkaloids with $-\text{COOH}$ and free $-\text{OH}$ surface groups [10, 11]. Various contaminants in water such as heavy metals, anions, pesticides, and dyes have been

removed by *Strychnos potatorum* seeds [12–18]. Nevertheless, there are only a few studies that are focused on the removal of contaminants using *Strychnos potatorum*-derived activated carbon (ACSP) [15].

The acrylamide monomer can be obtained by partial saponification of acrylonitrile. It is a colorless crystalline solid with high water solubility in water [19]. Polyacrylamide is obtained by free-radical polymerization of acrylamide, and polyacrylamide is used for the treatment of drinking water and wastewater. In addition, it is used in many other industrial processes, such as the production of dyes, paper, and plastics [19].

The treatment of water using *Strychnos potatorum*-derived activated carbon should be conducted in a suspended solution, which will result in a turbid and viscous solution at the end. Therefore, additional separation is needed to be conducted to remove the small particulate matter from the solution. This process may be difficult and probably expensive. In order to overcome this problem, it is better to produce composites with a robust polymeric material that has enhanced mechanical strength and durability [20]. Therefore, this study aims to determine the efficiency of ACSP-polyacrylamide composite in removing hardness in water. Adsorption isotherm, kinetics, and thermodynamic models were also used to describe the experimental equilibrium data.

2. Materials and Methods

2.1. Chemicals. All the chemicals that were used in this experiment were purchased from Sigma-Aldrich Chemical Company. H₂SO₄ (9.0 M, 15.0 mL), acrylamide (99%), and potassium persulphate (0.7 wt%) initiator were used in the composite preparation.

Furthermore, for the preparation of Ca and Mg solution, CaCl₂·H₂O (99%, ACS) and Mg(NO₃)₂·6H₂O (99%, ACS) chemicals were used. Moreover, NaOH (98%, ACS) and/or (37 wt. %, ACS) were used for the pH adjustment.

2.2. Preparation of Adsorbent

2.2.1. Synthesis of *Strychnos potatorum* Derived Activated Carbon (ACSP). Raw *Strychnos potatorum* seeds were purchased from an Ayurvedic shop in Sri Lanka and washed thoroughly with hot distilled water to remove all impurities. The seeds were air-dried for 24 hours at 105°C. For the preparation of activated carbon of *Strychnos potatorum* seeds, H₂SO₄ (9.0 M, 15.0 mL) solution was poured into dried seeds (125g). Then, the mixture was carbonized in a muffle furnace at 400°C for 15 min. The activated *Strychnos potatorum* seeds were washed with deionized water several times until the pH of the washing solution reaches 6-7 and oven-dried for 24 hrs at 105°C. Then, dried ACSP was crushed and sieved using a 250 μm sieve.

2.2.2. Synthesis of Polyacrylamide-*Strychnos potatorum* Derived Activated Carbon Composite (PA-ACSPC). For the synthesis of *Strychnos potatorum*-derived activated carbon

composite (PA-ACSPC), 8.0 g of acrylamide was weighed and dissolved in 28 mL of deionized water. Then, *Strychnos potatorum*-derived activated carbon (6 g) was added and stirred for 1 hr (200 rpm). The mixture was purged with N₂ for 15 minutes. A potassium persulphate (0.7 wt%) initiator was added, and the mixture was kept in a 55°C water bath to allow the polymerization to occur. The reaction was continued for 1 hour to complete the polymerization. Then, the synthesized polymer composite was removed and washed with acetone. It was dried for 5 hours in an air oven at 50°C and placed in a desiccator. The dried composite was crushed using laboratory mortar and pestle before taking for the adsorption experiments.

2.3. Characterization of the Adsorbent. PA-ACSPC, pure polyacrylamide, and *Strychnos potatorum*-derived activated carbon were analyzed using Fourier transform infrared (FTIR) spectrometer (PerkinElmer Corporation, Norwalk, CT) to evaluate the functional groups which were responsible for adsorption and to investigate vibration frequency changes. Furthermore, the surface morphology of synthesized PA-ACSPC was examined by scanning electron microscopy (VEGA3 SEM, TESCAN).

2.4. Batch Experiments. Batch adsorption experiments were carried out in a 250 mL glass conical flask by shaking 0.5 g of PA-ACSPC adsorbents in a 50 mL of Ca/Mg solution mixture of pH 7 on a shaking incubator at 200 rpm for 3 hours at 25°C. The concentration of Ca and Mg in the mixture was 200 mg/L. Several operating parameters, including the effect of contact time (5–180 min), initial concentration (25–1000 mg/L), temperature (20–40°C), adsorbent dosage (0.05–2 g), and pH (3–8), were investigated in this study. The optimized adsorption time for this synthesized composite was first examined by varying the contact time at 25°C temperature, pH 7, and adsorbent dosage of 0.5 g in 50 mL of Ca (200 mg/L) and Mg (200 mg/L) solution mixture. Then, the pH was adjusted by adding NaOH or HCl solution. After the adsorption experiment, solutions were separated from the composite by centrifugation at 10,000 rpm for 15 min (MX-207, Tomy Seiko Co., Ltd. Tokyo, Japan). The calcium and magnesium concentrations were analyzed using flame atomic absorption spectroscopy (GBC Avanta, Australia). All experiments were carried out in duplicate, and the average value was taken for data analysis.

The removal efficiency (RE) was determined using the following equation:

$$RE = \frac{C_o - C_e}{C_o} \times 100, \quad (1)$$

where C_o is the initial concentration of the adsorbate (mg/L) and C_e is the equilibrium concentration of the adsorbate (mg/L).

2.5. Isotherm and Kinetic Experiments. Isotherm and thermodynamic and kinetics experiments were carried out using

0.5 g of each adsorbent in 50 mL of calcium/magnesium (1 : 1) mixture at pH 7 by shaking at 200 rpm. In the isotherm experiments, the concentration range for both calcium and magnesium was 25–1000 mg/L and the equilibrium time was 120 min. Furthermore, in kinetic studies, equilibrium data were taken at time intervals of 5, 15, 30, 60, 70, 90, and 120 min, and the concentration of both calcium and magnesium was 200 mg/L. The temperature for both the isotherm and the kinetic experiment was 25°C. Moreover, according to the thermodynamic studies, the adsorption studies were conducted at four temperatures of 20, 25, 30, and 40°C (concentration of both calcium and magnesium was 200 mg/L and time was 120 min).

2.6. Field Studies. Several water quality complications were found in well water in the Anuradhapura district [21–23]. Among the water quality complications, high hardness content in well water is the most significant [22]. Therefore, water samples ($n=6$) were randomly collected from dug wells in the Medawachchiya Divisional Secretariat (DS) of Anuradhapura district, Sri Lanka, during the premonsoon season. The primary water quality parameters such as pH, dissolved solids (TDS), and electrical conductivity were obtained by a HACH HQ40d multiparameter meter (HACH, Loveland, Colorado, USA). Calcium and magnesium concentrations in water samples were determined by flame atomic absorption spectroscopy, and hardness was calculated using calcium and magnesium concentration according to APHA standards (APHA, 1998).

In order to investigate the removal efficiency of hardness by PA-ACSPC under field conditions, each water sample (50.0 mL) was treated with the synthesized PA-ACSPC (0.5 g) for 120 min at 200 rpm in a shaking incubator. The resulted equilibrated solution was obtained, and the remaining hardness was determined.

3. Results and Discussion

3.1. Characterization of PA-ACSPC

3.1.1. SEM Analysis. According to Figure 1(a), *Strychnos potatorum* seed powder did not have many unique features. It seemed to have an amorphous structure. However, the surface of charcoal prepared from *Strychnos potatorum* seeds had a porous structure with a smooth surface and had lost its amorphous structure giving it much more rigidity (or microcrystalline nature) compared to *Strychnos potatorum* seed powder. Furthermore, oval- and circular-shaped pores were observed (Figure 1(b)). Furthermore, the surface of activated carbon prepared from *Strychnos potatorum* seeds consisted of a highly porous, crystalline structure. These structures seemed to have a network of pores that were connected. Some pores seemed hexagonal in shape (Figure 1(c)). The surface of PA-ACSPC consisted of a rough surface having incomplete holes/shallow cavity-like structures, and these holes/cavities-like structures looked circular, oval, and irregular in shape due to the coverage by the polymer (Figure 1(d)).

3.1.2. FTIR Analysis. Figure 2 represents the FTIR spectra of PA, ACSP, and PA-ACSPC adsorbents. In the FTIR spectra of PA and PA-ACSPC, the peak around 2937 cm^{-1} is due to the C–H stretching of CH_2 moiety. Furthermore, the peaks at 1652 and 3344 cm^{-1} are due to C = O and N–H moieties [24]. In addition, in the spectra of PA and PA-ACSPC, the band at 1454 cm^{-1} is due to C–O stretching vibrations. The FTIR spectrum of the PA-ACSPC consisted of bands from both the ACSP and PA. Therefore, this indicated the co-existence of networks of ACSP and PA in the synthesized PA-ACSPC.

3.2. Effect of Contact Time. The effect of contact time on the removal of Ca and Mg ions and total hardness is shown in Figure 3. Hardness was calculated according to the APHA standards (APHA -2340B) (APHA, 1998). Observation revealed that the removal of ions responsible for hardness increased with increasing contact time. The rates of adsorptions of all three parameters were very high at the start and had approached the equilibrium within 2 hours. Furthermore, an increase in the contact time had not shown significant removal of Ca and Mg ions in solution.

The number of vacant surface sites in an adsorbent is fixed. Therefore, adsorption is fast during the initial stage, and the adsorption rate decreases with the decrease in the available active sites of the adsorbent [25]. Moreover, due to some repulsive forces that were generated between solutes in the solid and liquid phases, the adsorption rate may be decreased with time [2].

3.3. Effect of Concentration. The effects of initial Ca and Mg ion concentrations and the respective total hardness content for the removal efficiency were investigated while maintaining the adsorbent dosage at 0.5 g and pH at 7.0. The pattern of adsorption capacity (q_e) and percentage removal varied with the initial Ca and Mg ion contents, as shown in Figure 4. The adsorption capacity of calcium, magnesium, and the removal of total hardness increased with increasing the initial concentrations. In this study, the effect of initial concentrations was investigated up to 1000 mg/L of Ca and Mg ion concentrations. Up to that point, the adsorption capacity of PA-ACSPC has not become constant. Moreover, the percentage removals of calcium and magnesium ions and hardness contents are calculated, and the results are shown in Figure 4.

3.4. Effect of Adsorbent Dosage. The effect of adsorbent dosage on the percentage removal of Ca and Mg ions and the respective hardness is shown in Figure 5. The effect of adsorbent dosage was investigated at different adsorbent dosages of 0.05–1.00 g while keeping the Ca and Mg concentrations and the volume of the solution mixture constant. According to the results, the percentage of adsorption increased with adsorbent dosage. This was due to the increase in the available active sites of the adsorbent [26, 27]. The maximum removals of all parameters were observed at an optimum dosage of 0.5 g. The removal of Ca and Mg ions

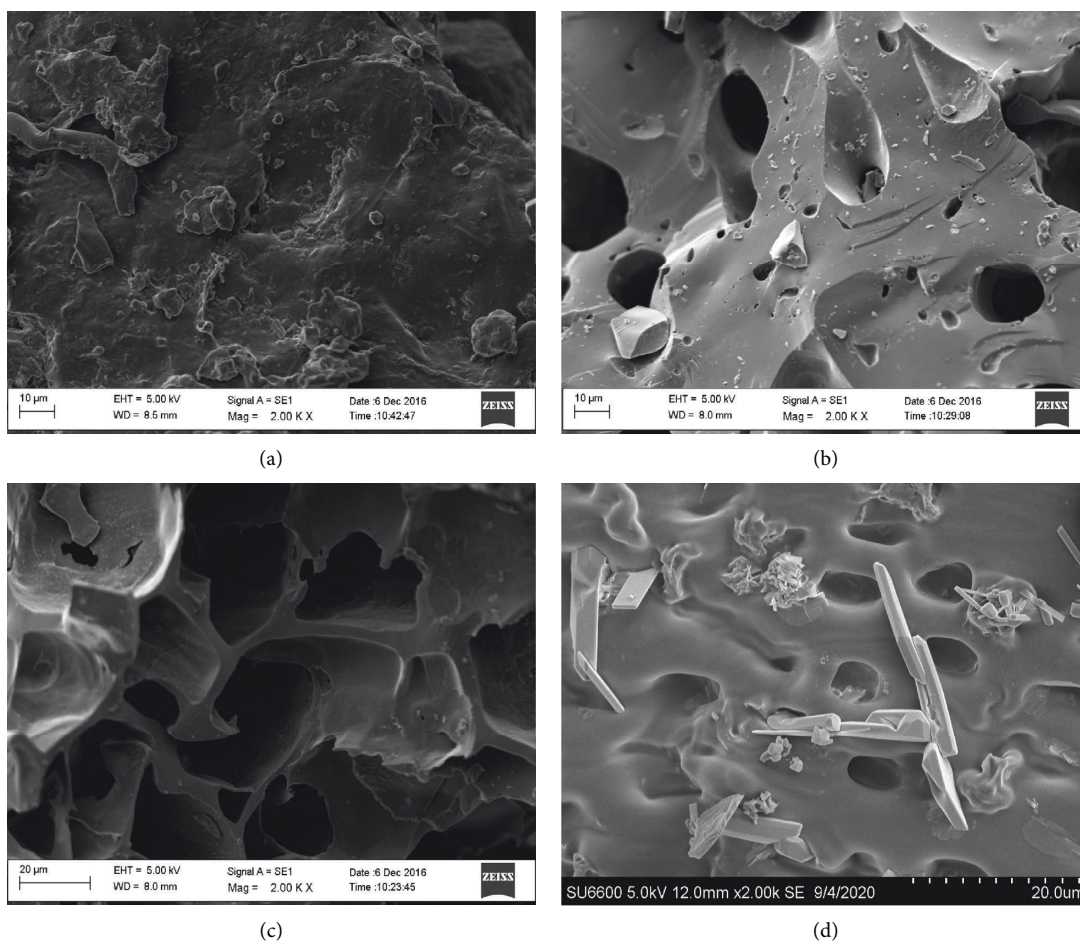


FIGURE 1: SEM images of (a) *Strychnos potatorum* seed powder, (b) charcoal prepared from *Strychnos potatorum* seeds, (c) activated carbon prepared from *Strychnos potatorum* seeds, and (d) PA-ACSPC.

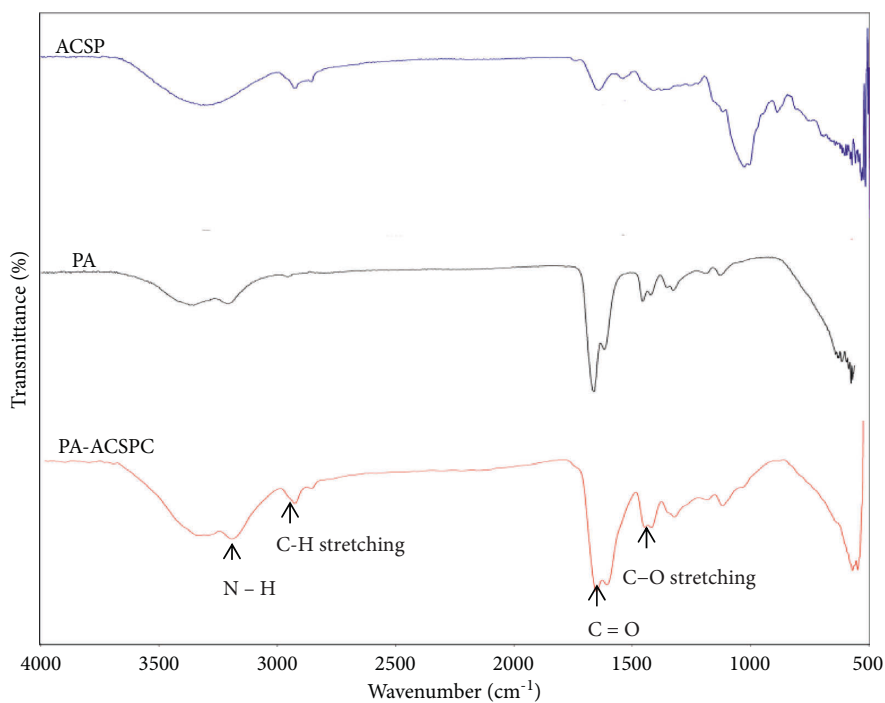


FIGURE 2: FTIR spectra of ACSP, PA, and PA-ACSPC samples.

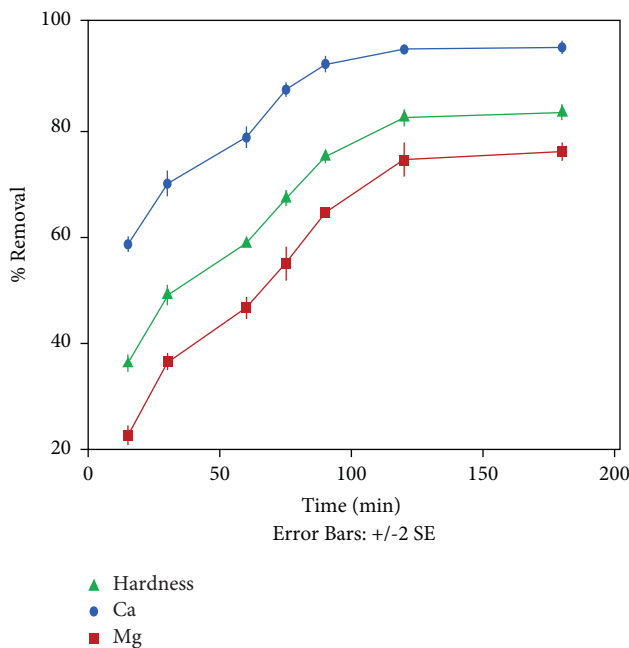


FIGURE 3: Effect of contact time.

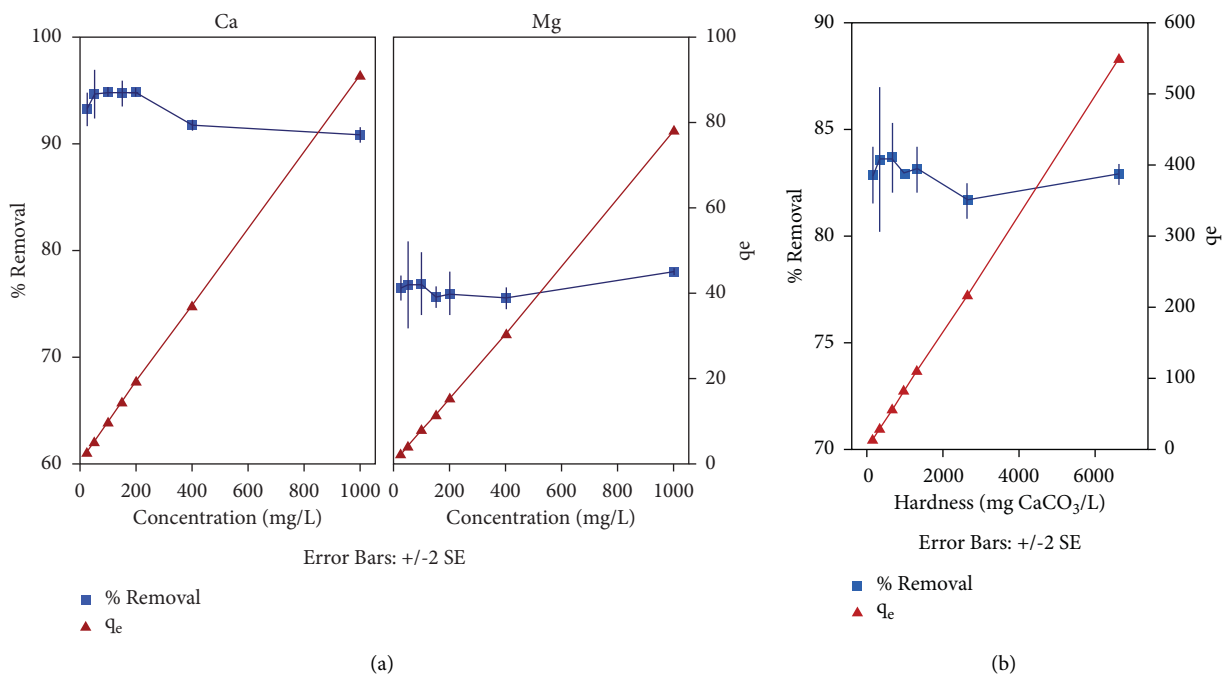


FIGURE 4: Effect of (a) concentration of calcium and magnesium ions and (b) content of hardness.

became almost constant beyond this adsorbent dosage. This may be attributed to the reduction in the Ca and Mg ion concentration gradients between the solution and the adsorbent surface [28].

3.5. Effect of pH. The percentage removal of Ca and Mg ions and hardness by PA-ACSPC at different pH values is presented in Figure 6. According to the results, all three parameters

showed similar behavior with pH. The % removals were slightly higher in alkaline conditions compared to the ambient pH values. This may be due to precipitation/colloid formation of metal hydroxides. The exact reason for the variation of the percentage removal of each parameter at low and intermediate pH values cannot be made due to the complex structure and chemical modifications of the adsorbent under the above conditions. However, a considerable Ca, Mg, and total hardness removal had been obtained at all pH values.

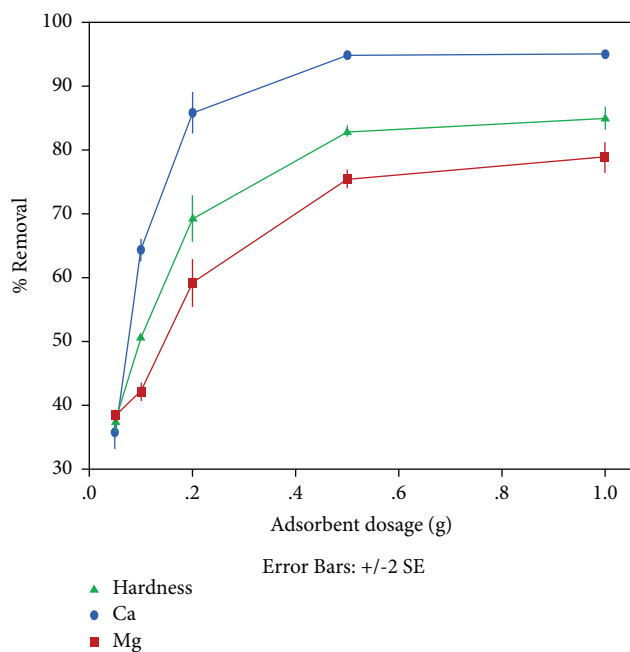


FIGURE 5: Effect of adsorbent dosage.

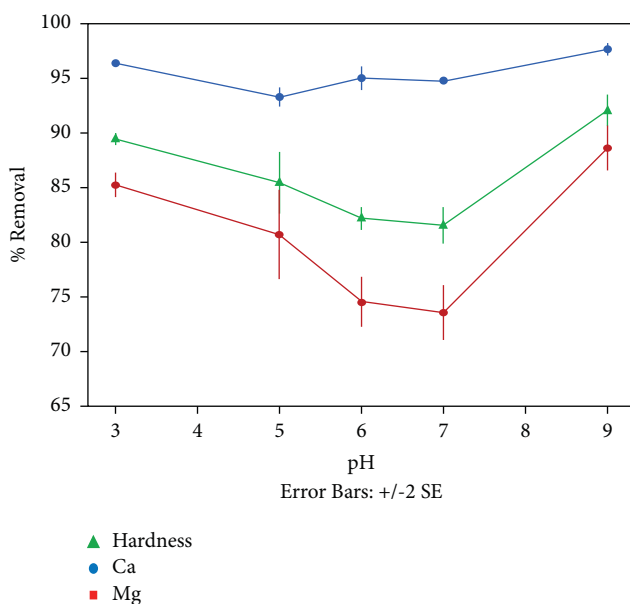


FIGURE 6: Effect of pH.

3.6. Sorption Isotherms of Ca and Mg ions on PA-ACSPC.

The adsorption capacities of PA-ACSPC for Ca and Mg ions and the respective hardness at different concentrations (25–1000 mg/L) were tested in order to investigate the removal mechanisms based on Langmuir and Freundlich isotherm models. These isotherm studies were carried out using a fixed amount of adsorbent (0.5 g) in 50 mL of the solution of pH 7 at 25°C by shaking at 200 rpm for 2 hrs.

The amount of Ca and Mg retained in the adsorbent phase was calculated using equation (2). The nonlinear form of the Langmuir isotherm model is expressed with equation

(3). Langmuir model describes homogeneous and independent monolayer adsorption, which was proposed by Irving Langmuir in 1916 [29]. Freundlich adsorption isotherm is an empirical model that can be applied to multilayer adsorption on a heterogeneous surface [30]. The nonlinear form of the Freundlich isotherm model is expressed with equation (4). The OriginPro v9.5 software was used for fitting experimental data to isotherm models:

$$q_e = (C_o - C_e)VM^{-1}, \quad (2)$$

$$q_e = \frac{K_L C_e}{1 + q_{\max} C_e}, \quad (3)$$

$$q_e = K_F C_e^{n_F}, \quad (4)$$

where q_e is the amount of adsorbate adsorbed per Gram of the adsorbent at the equilibrium (mg/g), C_o is the initial concentration of the adsorbate (mg/L), C_e is the equilibrium concentration of the adsorbate (mg/L), V is the volume of the solution mixture (L), and M is the adsorbent dosage (g). In equation (3), q_{\max} is the maximum monolayer coverage capacity (mg/g) and K_L is the Langmuir isotherm constant (L/mg). Freundlich isotherm parameters of n_F and K_F (mg/g) are related to the intensity of adsorption and adsorption capacity, respectively [30].

Based on correlation coefficients, the results were well fitted to the Freundlich isotherm model for Ca and Mg ions and calculated hardness contents than the Langmuir isotherm model (Table 1) (Supplementary Information 1). Previous studies also reported similar behavior for hardness removal [31]. According to the Freundlich isotherm model, adsorption was not restricted to monolayer adsorption, and adsorption was happening on heterogeneous and amorphous surfaces [32]. The Freundlich parameter of n indicates the favorability of the adsorption process. Since the value of $1/n$ was less than one for hardness removal, the adsorption can be considered favorable [33].

3.7. Adsorption Thermodynamics. To evaluate the thermodynamic feasibility and to assess the spontaneous nature of the adsorption process, adsorption thermodynamic parameters such as free energy change (ΔG°), enthalpy change (ΔH°), and entropy change (ΔS°) were calculated.

The Gibbs free energy change (ΔG°) value was obtained using the following equation:

$$\Delta G^\circ = -RT \ln K_C^0, \quad (5)$$

$$\ln(K_C^0) = \frac{\Delta S^\circ}{R} - \frac{\Delta H^\circ}{RT}, \quad (6)$$

where K_C^0 is the equilibrium constant and the value of K_C^0 is the ratio of the Ca and Mg ion amounts adsorbed on the PA-ACSPC at equilibrium (q_e , mg/g) to the remaining Ca and Mg ion concentration in the solution at equilibrium (C_e , mg/L) [25], T is the absolute temperature in Kelvin (K), and R is the universal gas constant. The Gibbs free energy change (ΔG) value was negative for hardness removal, indicating a

TABLE 1: Freundlich isotherm parameters of PA-ACSPC.

Parameter	Hardness	Mg	Ca
$K_F ((\text{mg}/\text{kg}) (\text{L}/\text{mg})^{1/n})$	387.1	209.4	249.3
n	1.031	1.097	0.794
R^2	0.999	0.998	0.995

TABLE 2: Thermodynamic parameters of Ca, Mg, and hardness for PA-ACSPC adsorbent: (a) Gibbs free energy (ΔG°), (b) enthalpy (ΔH°), and entropy (ΔS°).

Temperature	Gibbs free energy (ΔG°) (kJ)			
	Ca	Mg	Hardness	
20°C	-5.984	-2.414	-3.411	
25°C	-7.354	-2.915	-4.019	
30°C	-8.598	-3.497	-4.636	
40°C	-10.092	-4.076	-5.259	
ΔH° (kJ/mol)		ΔS° (J/mol/K)		
Ca	Mg	Hardness	Ca	Hardness
62.730	25.401	0.928	234.765	96.032
				3.381

TABLE 3: Kinetic parameters of PA-ACSPC.

Kinetic parameters		Ca	Mg	Hardness
		q_e (mg/g)	13.680	14.825
Pseudo-first-order kinetic model	$K_{1,ads}$ (min^{-1})	0.039	0.0190	0.0216
	R^2	0.906	0.926	0.902
	SEE	0.154	0.0836	0.0948
Pseudo-second-order kinetic model	q_e (mg/g)	20.781	20.525	131.106
	K_t	0.0035	0.000865	0.000249
	R^2	0.997	0.975	0.989
	SEE	0.156	0.481	0.0483

spontaneous nature of adsorption (Table 2) (Supplementary Information 2).

The ΔG° values increased with the increasing temperature from 20°C to 40°C (Table 2). Therefore, the adsorption is more favorable at higher temperatures. Moreover, the positive value of ΔH° indicated that the adsorption reaction was endothermic [28]. Furthermore, according to the positive value of ΔS° , the adsorption reaction was a spontaneous process.

3.8. Adsorption Kinetics. The adsorption kinetic analysis is based on the reaction kinetics of pseudo-first-order Lagergren rate and pseudo-second-order mechanisms. The pseudo-first-order Lagergren rate model equation is as follows:

$$\log(q_e - q_t) = \left(\frac{-K_{1,ads}}{2.303} \right) t + \log q_e, \quad (7)$$

where $K_{1,ads}$ (min^{-1}) is the pseudo-first-order rate constant, q_t (mg/g) is the amount of adsorbate adsorbed on the adsorbent at any time t , and q_e (mg/g) is the amount of adsorbate adsorbed on the adsorbent at the equilibrium. The values of q_e and $K_{1,ads}$ can be determined by the intercept and slope of the plot.

The pseudo second-order model equation:

$$\frac{t}{q_t} = \frac{t}{q_e} + \frac{1}{k_t q_e^2}, \quad (8)$$

where K_t (mg/g.min) is the pseudo-second-order rate constant, and the values of K_t and q_e can be obtained by the slope and the intercept of the plot.

Experimental data were best fitted with a pseudo-second-order model according to the calculated R^2 values for calcium, magnesium, and hardness (Table 3) (Supplementary Information 3). Therefore, the obtained kinetic data suggested that the adsorption of Ca and Mg ion onto PA-ACSPC followed the pseudo-second-order model.

3.9. Field Study. The analyzed basic water quality parameters of the water samples collected from dug wells in Anuradhapura, Sri Lanka, are tabulated in Table 4.

After treating the well water samples with PA-ACSPC adsorbent, the hardness content of collected well water samples was successfully reduced (85–90%) (Table 5). According to the local standards, drinking water's recommended level of hardness is 250 mg CaCO_3/L [34]. Therefore, it can be concluded that PA-ACSPC can be used as a cost-effective, high-performing hardness removal agent in aqueous systems.

TABLE 4: Basic water quality parameters of collected well water samples.

Sample	pH	TDS (mg/L)	Conductivity ($\mu\text{S}/\text{cm}$)
1	6.70 \pm 0.14	371.0 \pm 2.8	770.0 \pm 9.9
2	6.96 \pm 0.37	656.0 \pm 5.7	1330.0 \pm 12.7
3	7.78 \pm 0.17	625.0 \pm 5.7	1234.0 \pm 5.7
4	6.28 \pm 0.03	279.5 \pm 16.3	587.2 \pm 2.5
5	7.33 \pm 0.10	479.0 \pm 7.1	997.3 \pm 2.4
6	7.22 \pm 0.17	508.0 \pm 7.1	1045.0 \pm 7.1

TABLE 5: Hardness of well water samples before and after treatment with the adsorbent PA-ACSPC.

Sample no.	Initial contents			Contents after treatment with PA-ACSPC			
	Ca (mg/L)	Mg (mg/L)	Hardness (mg CaCO_3/L)	Ca (mg/L)	Mg (mg/L)	Hardness (mg CaCO_3/L)	Percentage removal of hardness
1	230.260 \pm 0.766	250.678 \pm 0.180	1607.251 \pm 2.652	2.865 \pm 0.272	50.765 \pm 8.771	216.204 \pm 36.797	86.54 \pm 2.29
2	560.231 \pm 0.629	178.543 \pm 0.474	2134.137 \pm 0.380	26.986 \pm 1.506	41.987 \pm 4.760	240.287 \pm 23.364	88.74 \pm 1.09
3	128.934 \pm 0.481	270.211 \pm 0.617	1434.677 \pm 1.341	1.021 \pm 0.141	38.231 \pm 3.233	159.985 \pm 12.960	88.81 \pm 0.90
4	202.938 \pm 0.033	198.265 \pm 0.051	1323.191 \pm 0.293	1.983 \pm 0.069	41.837 \pm 1.515	177.236 \pm 6.410	86.60 \pm 0.48
5	357.987 \pm 0.633	154.821 \pm 0.787	1531.446 \pm 1.661	2.901 \pm 0.146	38.032 \pm 1.571	163.860 \pm 6.834	89.30 \pm 0.45
6	156.843 \pm 0.042	197.345 \pm 0.300	1204.304 \pm 1.339	1.103 \pm 0.013	35.925 \pm 3.497	150.693 \pm 14.370	87.48 \pm 1.19

4. Conclusion

Investigations of the present study have shown that PA-ACSPC can be used to efficiently remove the hardness of the water. The removal efficiency was influenced by the pH, contact time, adsorbate concentration, temperature, and adsorbent dosage. The synthetic composite of PA-ACSPC reached the adsorption equilibrium in 120 minutes. Furthermore, the adsorption data were well fitted to the Freundlich isotherm and the pseudo-second-order kinetic models. Therefore, adsorption was not restricted to monolayer adsorption, and adsorption was happening on heterogeneous and amorphous surfaces. Since the value of $1/n$ was less than one, the adsorption can be considered favorable. Moreover, high temperatures favored the removal of hardness. Water samples collected from Anuradhapura, Sri Lanka, with high hardness contents were treated with this PA-ACSPC, and the results suggested that this adsorbent could be used as an effective hardness removal agent. Since the Gibbs free energy change (ΔG) value was negative for hardness removal, the adsorption indicated a spontaneous nature.

Data Availability

The data are available on request from the corresponding author.

Conflicts of Interest

The authors declare that they have no conflicts of interest.

Acknowledgments

This study was supported by the University Grant Commission, Sri Lanka, under the research grant (RP/03/SR/02/06/01/2016).

Supplementary Materials

Supplementary Information 1: determination of isotherms parameters. Supplementary Information 2: adsorption thermodynamics parameters. Supplementary Information 3: determination of adsorption kinetic parameters. (*Supplementary Materials*)

References

- [1] M. Muqeet, A. Khalique, U. A. Qureshi et al., "Aqueous hardness removal by anionic functionalized electrospun cellulose nanofibers," *Cellulose*, vol. 25, no. 10, 2018.
- [2] C. Rolence, "Water hardness removal by coconut shell activated carbon," *International Journal of Science, Technology and Society*, vol. 2, no. 5, p. 97, 2014.
- [3] Y. Takahashi and Y. Imaizumi, "Hardness in drinking water," *Eisei Kagaku*, vol. 34, no. 5, pp. 475–479, 1988.
- [4] M. K. Ahn and C. Han, "Technologies for the removal of water hardness and scaling prevention," *Journal of Energy Engineering*, vol. 26, no. 2, pp. 73–79, 2017.
- [5] J. N. Apell and T. H. Boyer, "Combined ion exchange treatment for removal of dissolved organic matter and hardness," *Water Research*, vol. 44, no. 8, 2010.
- [6] S. E. H. Comstock and T. H. Boyer, "Combined magnetic ion exchange and cation exchange for removal of DOC and hardness," *Chemical Engineering Journal*, vol. 241, pp. 366–375, 2014.
- [7] M. Malakootian and N. Yousefi, "The efficiency of electrocoagulation process using aluminum electrodes in removal of hardness from water," *Journal of hazardous materials*, vol. 6, no. 2, pp. 131–136, 2009.
- [8] W. Liu, R. P. Singh, S. Jothivel, and D. Fu, "Evaluation of groundwater hardness removal using activated clinoptilolite," *Environmental science and pollution research international*, vol. 27, 2019.
- [9] P. S. Kumar, K. N. Vaibhav, S. Rekhi, and A. Thyagarajan, "Removal of turbidity from washing machine discharge using *Strychnos potatorum* seeds: parameter optimization and

- mechanism prediction,” *Resource-Efficient Technologies*, vol. 2, 2016.
- [10] S. Vishali and R. Karthikeyan, “A comparative study of *Strychnos potatorum* and chemical coagulants in the treatment of paint and industrial effluents an alternate solution,” *Separation Science and Technology*, vol. 49, no. 16, 2014.
- [11] K. Grace Pavithra, P. Senthil Kumar, F. Carolin Christopher, and A. Saravanan, “Removal of toxic Cr(VI) ions from tannery industrial wastewater using a newly designed three-phase three-dimensional electrode reactor,” *Journal of Physics and Chemistry of Solids*, vol. 110, pp. 379–385, 2017.
- [12] M. B. Abou-Donia and A. W. Abu-Qare, “Simultaneous determination of chlorpyrifos, permethrin, and their metabolites in rat plasma and urine by high-performance liquid chromatography,” *Journal of Analytical Toxicology*, vol. 25, no. 4, pp. 275–279, 2001.
- [13] T. D. Fernando, Y. L. N. M. Arachchige, and W. N. C. P. Nawarathne, “Adsorption of diazinon residues from water by *Strychnos potatorum* seed flakes: equilibrium isotherm and thermodynamic analysis,” *Indian Journal of Science and Technology*, vol. 14, no. 6, pp. 573–581, 2021.
- [14] N. Gandhi and K. B. C. Sekhar, “Bioremediation of waste water by using *Strychnos potatorum* seeds (clearing nuts) as bio adsorbent and natural coagulant for removal of fluoride and chromium,” *Journal of International Academic Research for Multidisciplinary*, vol. 2, no. 1, pp. 253–272, 2014.
- [15] G. Muthuraman, “Kinetic studies for chromium (VI) removal by using *strychnos potatorum* seed powder and fly ash,” 2015, https://www.researchgate.net/publication/315667454_Kinetic_Studies_for_Chromium_VI_removal_by_using_Strychnos_potatorum_Seed_powder_And_Fly_ash.
- [16] B. Rajalakshmi and A. Jenifer, “Effective removal of nitrate from potable water of kodaikanal hills using-natural coagulant,” *International Journal of Informative and Futuristic Research*, vol. 2, no. 1, 2014.
- [17] N. C. Rani and M. V. Jadhav, “Enhancing Filtrate quality of turbid water incorporating seeds of *Strychnos potatorum*, pads of *Cactus opuntia* and mucilage extracted from the fruits of *Coccinia indica* as coagulants,” *Journal of Environmental Research & Development*, vol. 7, no. 2, pp. 668–674, 2012.
- [18] P. Senthil Kumar, C. Senthamarai, A. S. L. Sai Deepthi, and R. Bharani, “Adsorption isotherms, kinetics and mechanism of Pb(II) ions removal from aqueous solution using chemically modified agricultural waste,” *Canadian Journal of Chemical Engineering*, vol. 91, no. 12, 2013.
- [19] W. M. Kulicke, R. Kniewske, and J. Klein, “Preparation, characterization, solution properties and rheological behaviour of polyacrylamide,” *Progress in Polymer Science*, vol. 8, no. 4, pp. 373–468, 1982.
- [20] Z. Wan, D. Chen, H. Pei et al., “Batch study for Pb²⁺ removal by polyvinyl alcohol-biochar macroporous hydrogel bead,” *Environmental Technology*, vol. 42, no. 4, pp. 648–658, 2019.
- [21] T. D. Fernando, B. M. Jayawardena, and Y. L. Mathota Arachchige, “Variation of different metabolites and heavy metals in *Oryza sativa* L., related to chronic kidney disease of unknown etiology in Sri Lanka,” *Chemosphere*, vol. 247, Article ID 125836, 2020.
- [22] T. D. Fernando, Y. L. N. Mathota Arachchige, K. V. P. Sanjeevani, and R. A. M. T. S. Rajaguru, “Comprehensive groundwater quality analysis in chronic kidney disease of unknown etiology (CKDu) prevalence areas of Sri Lanka to investigate the responsible culprit,” *Journal of Chemistry*, pp. 1–10, 2022.
- [23] P. N. S. Pathirannehe, T. D. Fernando, and C. S. K. Rajapakse, “Removal of fluoride from drinking water using protonated glycerol diglycidyl ether cross-linked chitosan beads,” *Chemistry and Chemical Technology*, vol. 15, no. 2, pp. 205–216, 2021.
- [24] K. Zhang, Q. Wang, H. Meng, M. Wang, W. Wu, and J. Chen, “Preparation of polyacrylamide/silica composite capsules by inverse Pickering emulsion polymerization,” *Particuology*, vol. 14, pp. 12–18, 2014.
- [25] K. Jayaram, I. Y. L. N. Murthy, H. Lalhruaitluanga, and M. N. V. Prasad, “Biosorption of lead from aqueous solution by seed powder of *Strychnos potatorum* L.,” *Colloids and Surfaces B: Biointerfaces*, vol. 71, no. 2, pp. 248–254, 2009.
- [26] G. Moussavi, H. Hosseini, and A. Alahabadi, “The investigation of diazinon pesticide removal from contaminated water by adsorption onto NH₄Cl-induced activated carbon,” *Chemical Engineering Journal*, vol. 214, pp. 172–179, 2013.
- [27] M. Pirsahab, A. Dargahi, S. Hazrati, and M. Fazlzadehdavil, “Removal of diazinon and 2, 4-dichlorophenoxy-acetic acid (2, 4-D) from aqueous solutions by granular-activated carbon,” *Desalination and Water Treatment*, vol. 52, no. 22–24, 2014.
- [28] P. S. Kumar, R. Gayathri, C. Senthamarai et al., “Kinetics, mechanism, isotherm and thermodynamic analysis of adsorption of cadmium ions by surface-modified *Strychnos potatorum* seeds,” *Korean Journal of Chemical Engineering*, vol. 29, no. 12, 2012.
- [29] H. Swenson and N. P. Stadie, “Langmuir’s theory of adsorption: a centennial review,” *Langmuir*, vol. 35, no. 16, 2019.
- [30] R. Saadi, Z. Saadi, R. Fazaeli, and N. E. Fard, “Monolayer and multilayer adsorption isotherm models for sorption from aqueous media,” *Korean Journal of Chemical Engineering*, vol. 32, no. 5, pp. 787–799, 2015.
- [31] C. Rolence, “Adsorption studies on water hardness removal by using adsorption studies on water hardness removal by using cashewnut shell activated carbon,” *African Journal of Science and Research*, vol. 5, no. 4, pp. 78–81, 2016.
- [32] D. Mohan, S. Rajput, V. K. Singh, P. H. Steele, and C. U. Pittman, “Modeling and evaluation of chromium remediation from water using low cost bio-char, a green adsorbent,” *Journal of Hazardous Materials*, vol. 188, no. 1–3, pp. 319–333, 2011.
- [33] S. Rayappan, B. Jeyaprabha, and P. Prakash, *Defluoridization Using a Natural Adsorbent, Cissus*, *International Journal of Engineering Research and Applications*, vol. 4, no. 10, pp. 67–74, 2014.
- [34] SLS, “Drinking water standard—first revision,” 2013, <https://www.coursehero.com/file/35673881/DOC-20181113-WA0010pdf/>.